Article

Inhibition of 37/67kDa Laminin-1 Receptor Restores APP Maturation and Reduces Amyloid-β in Human Skin Fibroblasts from Familial Alzheimer's Disease

Antaripa Bhattacharya [1,†], Antonella Izzo [1,†], Nunzia Mollo [1,†], Filomena Napolitano [2], Adriana Limone [1], Francesca Margheri [3], Alessandra Mocali [3], Giuseppina Minopoli [1], Alessandra Lo Bianco [4], Federica Di Maggio [1,5], Valeria D'Argenio [5,6], Nunzia Montuori [2], Antonio Lavecchia [4] and Daniela Sarnataro [1,5,*]

[1] Department of Molecular Medicine and Medical Biotechnology, University of Naples "Federico II", Via S. Pansini 5, 80131 Naples, Italy; antaripa1210@gmail.com (A.B.); antonella.izzo@unina.it (A.I.); nunzia.mollo@unina.it (N.M.); adriana.limone1996@gmail.com (A.L.); giuseppina.minopoli@unina.it (G.M.); dimaggio@ceinge.unina.it (F.D.M.)

[2] Department of Translational Medical Sciences, University of Naples "Federico II", Via S. Pansini 5, 80131 Naples, Italy; filomena-napolitano88@hotmail.it (F.N.); nmontuor@unina.it (N.M.)

[3] Department of Experimental and Clinical Biomedical Sciences, University of Florence, 50134 Florence, Italy; francesca.margheri@unifi.it (F.M.); alessandra.mocali@unifi.it (A.M.)

[4] Department of Pharmacy, "Drug Discovery Lab", University of Naples "Federico II", Via D. Montesano 49, 80131 Naples, Italy; alessandra.lobianco8@gmail.com (A.L.B.); antonio.lavecchia@unina.it (A.L.)

[5] CEINGE-Biotecnologie Avanzate Scarl, Via G. Salvatore 486, 80145 Naples, Italy; dargenio@ceinge.unina.it

[6] Department of Human Sciences and Quality of Life Promotion, San Raffaele Open University, Via di Val Cannuta 247, 00166 Rome, Italy

* Correspondence: sarnatar@unina.it

† These authors contributed equally to this work.

check for
updates

Abstract: Alzheimer's disease (AD) is a fatal neurodegenerative disorder caused by protein misfolding and aggregation, affecting brain function and causing dementia. Amyloid beta (Aβ), a peptide deriving from amyloid precursor protein (APP) cleavage by-and γ-secretases, is considered a pathological hallmark of AD. Our previous study, together with several lines of evidence, identified a strict link between APP, Aβ and 37/67kDa laminin receptor (LR), finding the possibility to regulate intracellular APP localization and maturation through modulation of the receptor. Here, we report that in fibroblasts from familial AD (fAD), APP was prevalently expressed as an immature isoform and accumulated preferentially in the transferrin-positive recycling compartment rather than in the Golgi apparatus. Moreover, besides the altered mitochondrial network exhibited by fAD patient cells, the levels of pAkt and pGSK3 were reduced in respect to healthy control fibroblasts and were accompanied by an increased amount of secreted Aβ in conditioned medium from cell cultures. Interestingly, these features were reversed by inhibition of 37/67kDa LR by NSC47924 a small molecule that was able to rescue the "typical" APP localization in the Golgi apparatus, with consequences on the Aβ level and mitochondrial network. Altogether, these findings suggest that 37/67kDa LR modulation may represent a useful tool to control APP trafficking and Aβ levels with implications in Alzheimer's disease.

Keywords: Alzheimer's disease; amyloid-β; amyloid precursor protein APP; NSC47924; 37/67kDa laminin-1 receptor inhibitor

1. Introduction

Extracellular amyloid plaques formed by deposits of Aβ peptide and intracellular neurofibrillary tangles, composed of hyperphosphorylated tau protein, represent the major neuropathologic event characterizing Alzheimer's disease (AD) [1].

Aβ derives from a sequential proteolytic cleavage of amyloid precursor protein (APP) by β- and γ-secretases. Mutations in Aβ, as well as in APP, near the β- and γ-secretase sites [2], together with duplication of the *APP* locus, give rise to AD [3]. The overwhelming majority of dominant mutations causing familial AD occurs in three genes: *APP*, *PSEN1* (*Presenilin-1*), and *PSEN2* (*Presenilin-2*). Interestingly, mutations in PSEN-1 and -2 have been described to increase the $A\beta_{42}/A\beta_{40}$ ratio [4,5].

To date, 19 different AD causing mutations in the γ-secretase enzyme PSEN-2 have been reported and were shown to alter the APP processing by increasing both the total level of Aβ and the $A\beta_{42/40}$ ratio [6,7], suggesting that the dysregulation of Aβ production from APP can be considered a common effect of these mutations.

In neurons, defects in APP trafficking and processing leading to Aβ production are likely the most common cause of AD; thus, understanding how APP is targeted to a defined cellular compartment and identifying the mechanisms that control the Aβ generation, could be a key for new therapies [8,9].

We have demonstrated that APP posttranslational modifications, strictly related to subcellular localization, and intracellular trafficking are extremely important for correct protein maturation and processing [10–15]. In this context, the already acknowledged role of 37/67kDa laminin receptor (LR) in the internalization and cytotoxicity of Aβ [16,17], together with our recent finding of its interaction with APP and its involvement in APP localization and maturation in neuronal cells [10], prompted us to analyze the effects of a specific inhibitor of 37/67kDa LR on the localization and processing of APP, as well as on Aβ generation, in fibroblast cell lines from familial AD patients compared with healthy unaffected ones.

We first characterized the absence of any pathogenic variant in *APP, PSEN1,* and *PSEN2* genes in one of the two cell lines from familial AD (here named fAD1). Then, we used another fibroblast cell line carrying the *PSEN2* M239V pathogenic mutation for familial AD (here named fAD3). Contrary to control fibroblasts (unAD, unaffected) where APP was localized in the Golgi apparatus, we found that in fAD fibroblast cell lines, APP lost its Golgi localization resulting mainly distributed in transferrin-positive recycling endosomes. The use of a specific inhibitor of 37/67kDa LR, NSC47924, completely rescued the localization of APP in the Golgi complex and restored the APP maturation, which was partially lost in fAD fibroblasts. In addition, the inhibitor was able to improve the mitochondrial network organization in terms of volume and number, to almost the same level of healthy individuals. Finally, the treatment with NSC47924 drastically reduced secreted Aβ levels in fAD fibroblasts culture media and inactivated Akt signaling with reduction of Ser9-pGSK3β, revealing the receptor a promising target for AD.

2. Results

2.1. Sanger Sequencing for APP, PSEN1 and PSEN2 in fAD1 Fibroblast Cell Line

To assess the presence of any pathogenic variant associated with AD onset, *APP*, *PSEN1*, and *PSEN2* genes' sequences were analyzed in a fAD1 fibroblast cell line (Methods). As shown in Table 1, two variants were found in *APP*, two in *PSEN1*, and nine in *PSEN2*.

All *APP* and *PSEN1* variants were in the non-coding regions; they were all classified as benign according to ACMG criteria. In *PSEN2*, we found 9 variants, of which 6 were intronic and 3 were exonic; the latter were all synonymous variants with no alteration at the protein level. No pathogenic variants were found in all 3 analyzed genes.

Table 1. List of DNA variants identified in *APP*, *PSEN1* and *PSEN2* by Sanger sequencing.

Gene	Exon	c.DNA	Protein	Genotype	rs	Clinvar	Varsome (DANN Score)	ACMG	Allelic Frequency *	HSF
APP	IVS10	c.1402–106A > G	-	HOM	rs440666	NA	0.29	Benign	0.71	-
	IVS11 A11	c.1530+79C > G	-	HOM	rs2251337	NA	0.39	Benign	0.88	-
PSEN1	IVS6	c.480+223A > G	-	HOM	rs214269	NA	0.58	Benign	0.73	No significant splicing motif alteration detected This mutation has probably no impact on splicing
	UTR	c.*2314delT	-	HOM	rs895744391	NA	-	Benign	0.01	-
PSEN2	4	c.69T > C	p.Ala23=	HOM	rs11405	Benign	0.39	Benign	0.76	-
	4	c.129C > T	p.Asn43=	HOM	rs6759	Benign	0.48	Benign	0.48	-
	IVS4	c.142–42G > A	-	HOM	rs1295643	NA	0.74	Benign	0.49	No significant splicing motif alteration detected This mutation has probably no impact on splicing
	IVS4	c.142–29T > C	-	HOM	rs1295644	NA	0.35	Benign	0.71	Alteration of an intronic ESS site Probably no impact on splicing
	5	c.261C > T	p.His87=	HOM	rs1046240	Benign	0.65	Benign	0.50	-
	IVS7	c.498+30G > C	-	HOM	rs2236910	NA	0.59	Benign	0.77	Creation of an intronic ESE site Probably no impact on splicing
	IVS9	c.887–24T > C	-	HOM	rs2802267	NA	0.41	Benign	0.75	Alteration of an intronic ESS site. Probably no impact on splicing. Creation of an intronic ESE site Probably no impact on splicing
	IVS11	c.1073–86A > G	-	HOM	rs10753428	NA	0.37	Benign	0.75	Creation of an intronic ESE site Probably no impact on splicing
	IVS12	c.1191+24G > A	-	HOM	rs2855562	NA	0.53	Benign	0.54	No significant splicing motif alteration detected This mutation has probably no impact on splicing

rs: reference SNP; DANN: Deleterious Annotation of Genetic Variants; ACMG: American College of Medical Genetics; HSF: Human Splicing Finder (http://www.umd.be/HSF/HSF.shtml); IVS: InterVening Sequence; HOM: homozygous; NA: not available; UCV: unclassified variant. * based on gnomAD Genomes, version: 2.1.1.

Recent studies report that causative gene mutations associated with familial AD, have been identified in *APP, PSEN1,* and *PSEN2.* However, mutations in these genes explain just a small percentage of all fAD cases. This finding suggests the existence of other, inherited, disease-predisposing genes [18]. Since we did not find any mutation in the main candidate genes (*APP, PSENs*), further experimentations will be needed to search for gene/s possibly involved in the fAD1 phenotype.

2.2. Mature/Immature APP Isoform Ratio Is Reduced in fAD Fibroblasts and NSC47924 Restores APP Isoform Ratio to That of unAD Fibroblasts

Since APP trafficking through the secretory pathway is a warranty for proper protein maturation, which in turn is crucial for protein processing [19], to analyze APP expression level and posttranslational modifications, we employed human skin fibroblasts from familial fAD1 and fAD3 individuals (see Materials and Methods for a detailed description).

As expected from the analysis of SDS-PAGE gel electrophoresis [10], the APP migrated as two different bands corresponding to immature (~100 kDa) and mature glycosylated isoform (~130 kDa) (Figure 1).
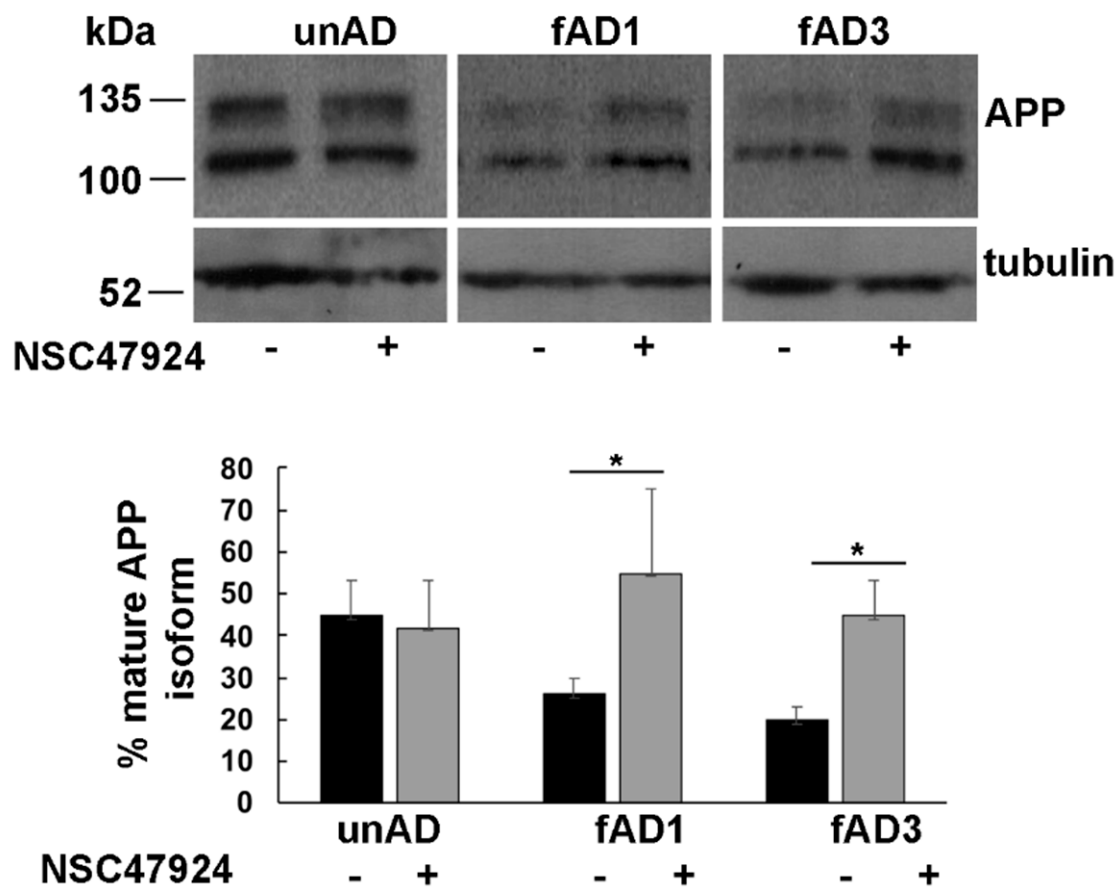

Figure 1. Inhibition of 37/67kDa LR by NSC47924 restored the amyloid precursor protein (APP) isoform ratio in fAD fibroblasts. Cultured fAD1, fAD3 and unAD fibroblasts were scraped in lysis buffer and 40 μg of total proteins were subjected to SDS-PAGE. APP was revealed by Western blotting on PVDF (Polyvinylidene Difluoride membranes) and hybridization with the A8717 antibody. fAD1, fAD3, and unAD fibroblasts were treated with NSC47924 for 24 h. Protein levels of mature APP were calculated by densitometric analysis with ImageJ software and expressed as a percentage. The plot shows the percentage of mature APP isoform, using 100% as the sum values of immature plus mature isoform with respect to tubulin as a loading control, under treated or not treated conditions. Data are expressed as the means + SD of three independent experiments (* $p < 0.05$).

Densitometric analysis of bands obtained by western blotting procedure with anti-APP antibody was performed to quantify the ratio between APP isoforms. The percentage of mature APP, with respect to total bands, is reported in the lower panel of Figure 1.

By using tubulin as a loading control, we found that the mature/immature APP ratio was significantly lower in both fAD fibroblast cell lines (0.26 ± 0.04 in fAD1 and 0.20 ± 0.03 in fAD3) with respect to the unAD controls (0.42 ± 0.08, $p < 0.05$), indicating that the APP was not able to completely mature along the secretory pathway, where normally it should traffic [20]. Incubation of cells with NSC47924 inhibitor, significantly rescued the APP ratio values (0.55 ± 0.2 in fAD1 and 0.45 ± 0.08 in fAD3, versus 0.45 ± 0.1 in unAD) (Table 2), strongly suggesting the molecule is working possibly by "correcting" the trafficking of the APP in mutant cells.

Table 2. Mature/Immature APP isoform ratio.

	Untreated	**NSC47924 (20 μM)**
unAD	0.42 ± 0.08	0.45 ± 0.1
fAD1	0.26 ± 0.04	0.55 ± 0.2
fAD3	0.20 ± 0.03	0.45 ± 0.08

The fact that the inhibitor effects were elicited both in fAD1, where no pathogenic *APP* or *PSEN* mutations were found, and in fAD carrying pathogenic *PSEN2* mutation, indicates that localization of the APP was independent of the expression of wild-type or mutated PSENs.

2.3. APP Is Mainly Localized in Recycling Endosomes Rather than in the Golgi Apparatus in fAD Fibroblasts

Our finding that APP was not completely mature in fAD cells, led us to speculate that APP was not able to be modified in the Golgi apparatus. Thus, to verify this hypothesis, we analyzed the intracellular distribution of APP in mutant cells, by employing fluorescence microscopy using different markers of the intracellular organelles. In agreement with previous observations in neuronal and non-neuronal cells [10,20,21], in control fibroblasts from unaffected donors, we found a significant colocalization of APP with Giantin, a marker of the Golgi complex (Pearson Correlation Coefficient, PCC = 0.86) (Figure 2).

On the contrary, in patient fibroblasts (both fAD1, Figure 3 and fAD2/3, Figures S1 and S2) APP lost its Golgi distribution to relocate into recycling endosomes (PCC = 0.92 for APP/Tfr), which were positive for Transferrin, a typical marker of recycling endosomes (Figure 3; Figures S1 and S2, upper panels, untreated).

Because we have previously described a link between APP subcellular localization/maturation and the 37/67kDa laminin receptor in neuronal cells [10], we tested the effects of a specific inhibitor of the receptor in fAD cells compared to unAD fibroblasts.

Interestingly, the use of NSC47924 inhibitor [22] restored the localization of APP in fAD fibroblasts relocating APP to the Golgi complex (Figures 2 and 3; Figures S1 and S2, bottom panels, NSC47924 treated, PCC = 0.88 for APP/Giantin). Consequently, after treatment with the inhibitor, the APP lost the colocalization with the recycling endosomes (Figures 2 and 3; Figures S1 and S2, bottom panels, PCC = 0.29 for APP/Tfr), which are critical intracellular compartments for peptide metabolism and protein function [23]. Thus, these results indicate that in AD fibroblasts, the "typical" Golgi APP intracellular localization is restored by a small molecule which is a specific inhibitor of the 37/67kDa LR.
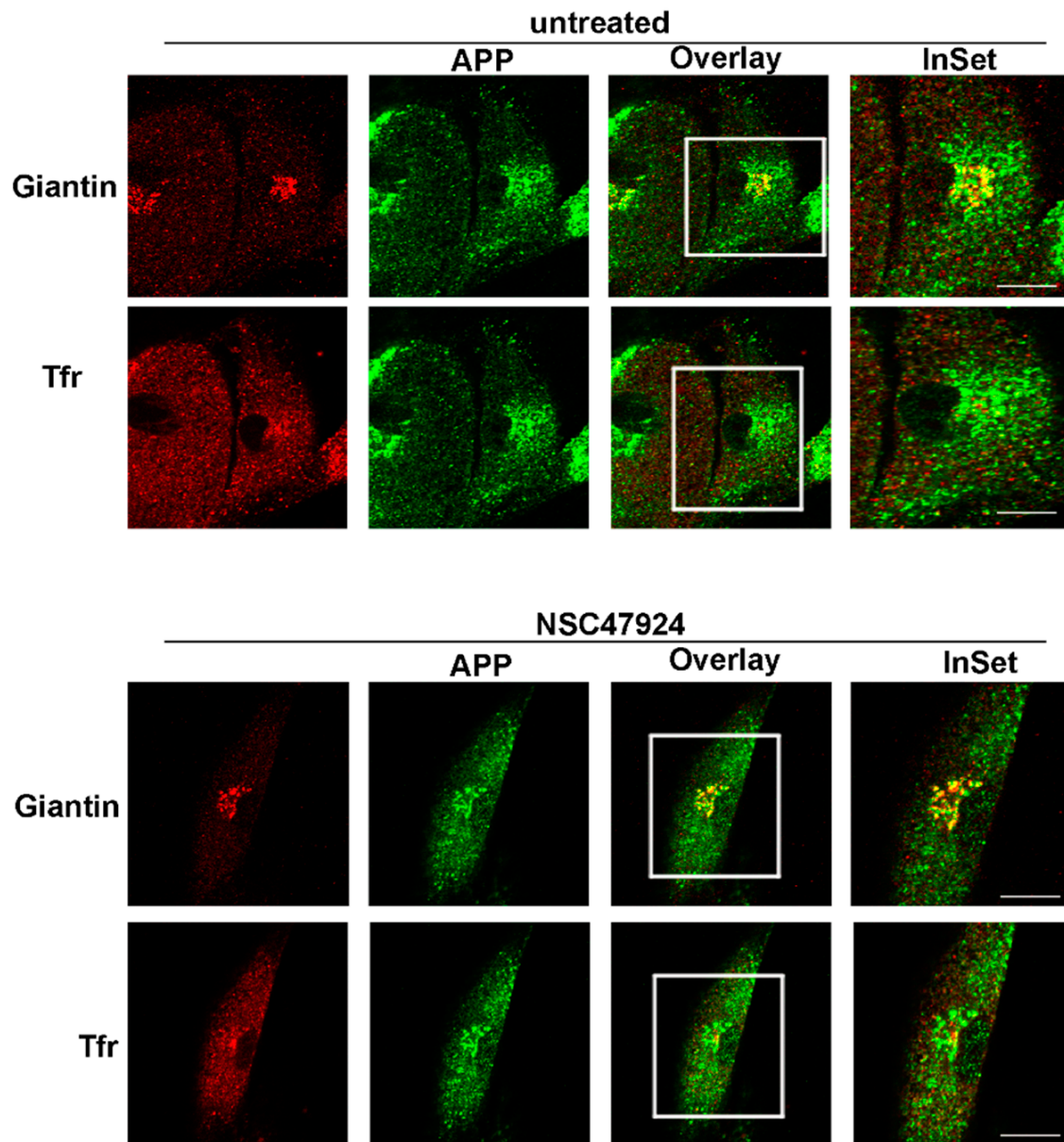
unAD fibroblasts

Figure 2. APP is localized in the Golgi apparatus in control unAD fibroblasts. Cells were grown on coverslips, fixed in PFA 4% and permeabilized in 0.1% TX-100 for 30 min, then they were stained by double immunolabeling with A8717 rabbit antibody (1:500) and Giantin (1:50), followed by cy2- and cy5-conjugated secondary antibodies, to label APP (green) and Golgi (red), respectively. Tfr Alexa-594 (red) in the cell culture media was used to label recycling endosomes. Colocalization between APP and the different markers was then measured as indicated in the methods section. The color channels in the triple image acquisition, have been split into green, red and blue. The blue channel is attributed to the cy5-conjugated secondary antibody, for easier visualization of the overlay, it has been rendered red after channel splitting and picture acquisition. Images from NSC47924 treatment are shown in the bottom panel. Scale bars, 10 μm.
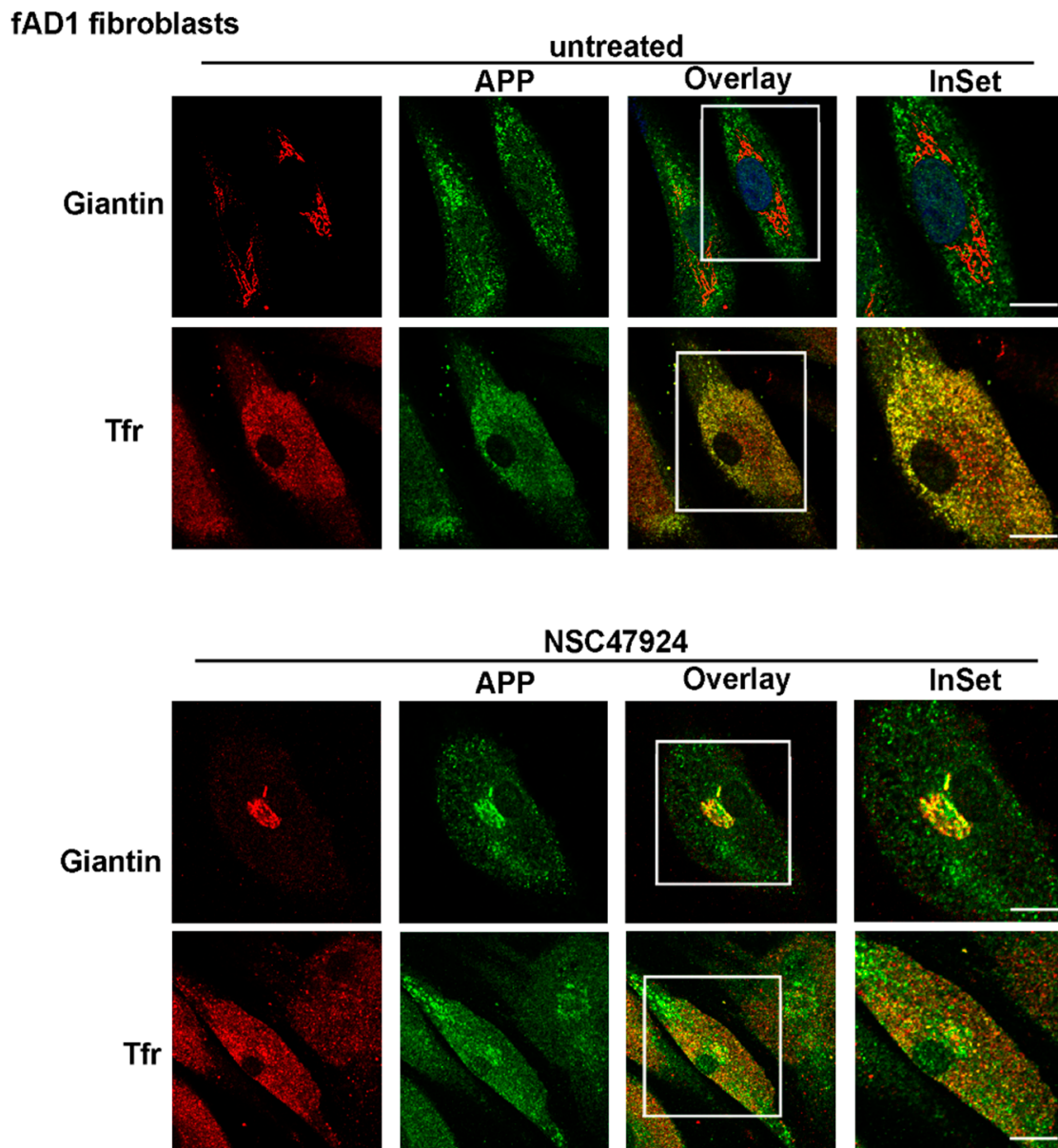
fAD1 fibroblasts

Figure 3. APP is mainly localized in Tfr-positive recycling endosomes in fAD1 fibroblasts. FAD1 cells were grown and processed for immunofluorescence as in Figure 2. Note the absence of APP in the Golgi apparatus and the presence in recycling endosomes in untreated fAD fibroblasts. Intracellular APP localization is reversed by NSC47924 incubation. Scale bars, 10 μm.

2.4. The Mitochondrial Network Is Compromised in fAD Fibroblasts and Improved by Inhibition of 37/67kDa LR

Because mitochondrial morphology and number [24], as well as mitochondrial biogenesis and transport along the neuronal axon [25], were found to be severely compromised in AD [26], as well as in aging and other neurodegenerative diseases [27,28], we analyzed the mitochondrial network organization in fAD fibroblasts. Because the mitochondrial function is linked to the organization of the mitochondrial network [29], we examined the mitochondrial morphology by using the Mitotracker Red CMXRos probe (Figure 4).
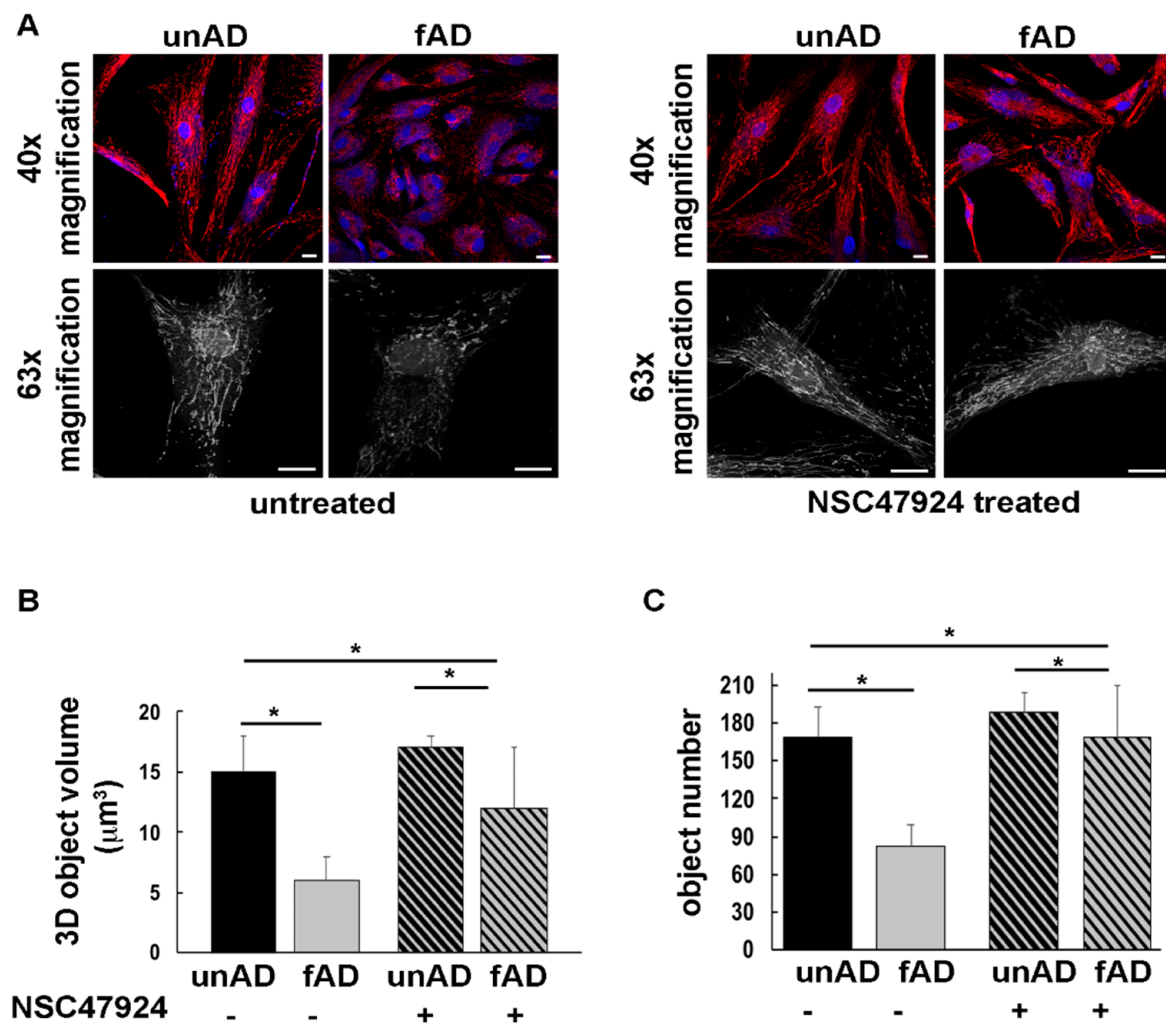
Figure 4. The mitochondrial network is altered in fAD fibroblasts and is restored by 37/67kDa LR inhibition by NSC47924. (**A**) UnAD (control) and fAD cells were seeded on glass coverslips and stained with the Mitotracker Red CMXRos probe for 20 min at 37 °C, then they were fixed and processed for immunofluorescence. Serial confocal sections were collected from top to bottom of one selected fAD cell line. Representative images of a single confocal plane (40× magnification, upper panels) and 3D reconstructions (black and white images, bottom panel) of Z-stack acquired to higher magnification (63×) are shown. Scale bars, 10 μm. (**B**) The average mitochondrial volume (expressed as 3D object volume, μm^3) is significantly higher in unAD cells compared with fAD cells. The bars show mean values + SD of two fAD and two unAD cell cultures. Fifteen randomly selected cells for each experimental condition were analyzed. NSC47924 was used as indicated in the methods section. (**C**) The number of mitochondria is significantly higher in unAD fibroblasts compared to fAD cells. Inhibition of the receptor by NSC47924 restored the parameters to that of unAD control ones (* $p < 0.05$).

The morphology of the mitochondrial network was profoundly altered in both fAD fibroblasts compared to unAD cells (Figure 4A). Three-dimensional (3D) reconstructions in the patient cells revealed that the mitochondrial network exhibited thinner and shorter tubules with respect to unAD cells, losing the typical interconnected tubular structure (Figure 4A). These data were strengthened by measuring the volume and number of mitochondria (Figure 4B,C), which were reduced in fAD compared to unAD, and then restored by the 37/67kDa LR inhibitor NSC47924 (Figure 4A, right panel, and Figure 4B,C).

2.5. Inhibitor Treatment Inactivates Akt Signaling with Consequent Activation of GSK3β Pathway

The mitochondrial pool of GSK3β has been involved in mitochondrial functions [30] and seems to be central in AD pathogenesis through changes in its phosphorylation state, as well as expression levels [31]. Starting from these observations, we investigated the phosphorylation status of GSK3β in Serine 9, which is indicative of GSK inactivation. In agreement with previous observation in neuronal cells [32], we found that pGSK3β levels were lower in fAD fibroblasts compared to unAD ones and that NSC47924 treatment decreased pGSK3β with respect to untreated samples (Figure 5A).
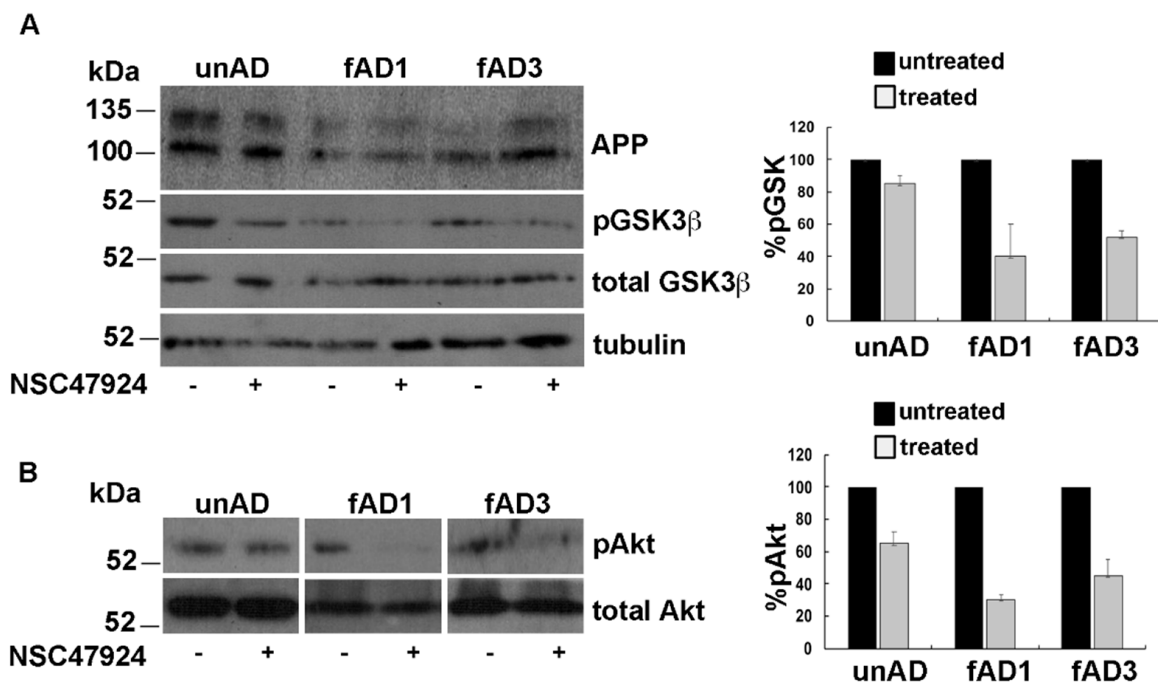

Figure 5. NSC47924 induces inactivation of Akt with the consequent decrement of pGSK3β. (**A**) Total cell lysates (40 μg) from unAD and fAD cells treated or not with NSC47924, were loaded on gels. Both total and pGSK3β levels were revealed by using anti-GSK3β and anti-phospho-Ser9 GSK3β antibody, respectively. (**B**) The membranes were treated as in (**A**) with the exception that here they were hybridized with anti-Akt and pAkt antibodies. The plots on the right show the percentage of pGSK and pAkt, using as 100% the values of pGSK3β and pAkt in the absence of the inhibitor. Data are expressed as the means + SD of three independent experiments (all data were statistically significant).

Furthermore, the analysis of Akt activation by western blot under NSC47924 treatment, revealed that pAkt was reduced with respect to untreated control conditions (Figure 5B).

2.6. The Amount of Secreted Aβ Is Significantly Higher in fAD Cells and Is Reduced by NSC47924 Treatment

The detection of Amyloid-β peptide and the identification of molecules capable to interfere with its generation, represent an important approach to study AD.

Herein, we analyzed by ELISA assays the levels of Aβ in conditioned media obtained from cultured skin fibroblasts of fAD patients and healthy controls (Figure 6). This analysis was conducted by ELISA assay because this method is able to capture Aβ species closer to their native conformation in vivo.
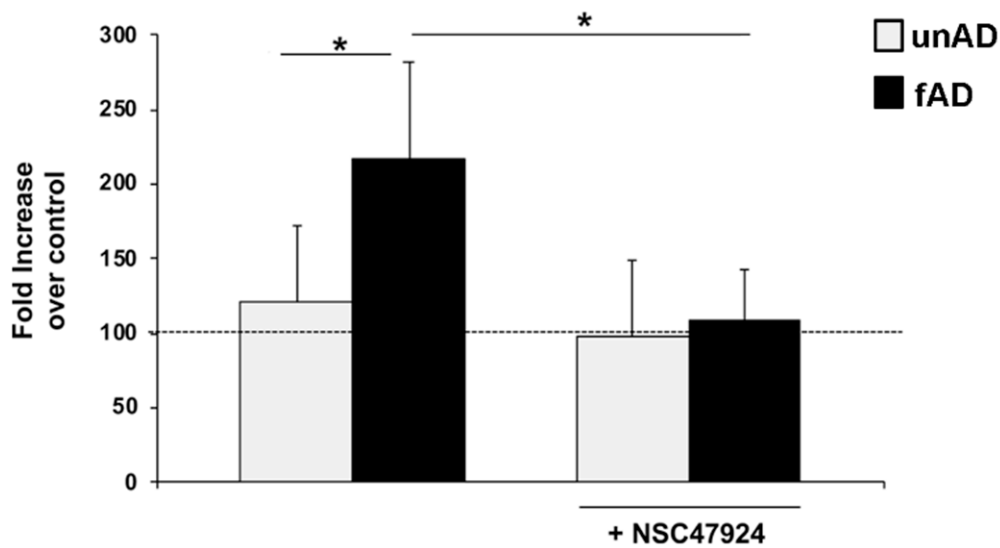
Figure 6. Aβ secreted levels are higher in fAD cell culture media and are decreased by inhibitor treatment. Conditioned medium from healthy (gray) and fAD (black) fibroblasts was incubated with an anti-Aβ monoclonal antibody (6E10) or non-immune control immunoglobulins IgG. The bound anti-Aβ antibody was revealed by OPD staining; the absorbance at 490 nm was measured. Anti-Aβ antibody binding to BSA-coated wells was subtracted to obtain a specific binding. Results are expressed as a percentage increase of anti-Aβ antibody absorbance value over non-immune control IgG, using as 100% the expression value in control conditions. Values represent the mean ± SEM of three experiments carried out in triplicate; (* $p < 0.05$).

The assay relies on the use of an anti-Aβ monoclonal antibody for capture. To increase the specificity of the ELISA, we utilized non-immune IgG as a control, and in two independent assays, two different antibodies specifically recognizing Aβ peptide (6E10 in Figure 6 and 4G8 in Figure S3). In parallel, anti-Aβ antibody binding to BSA-coated wells was also evaluated and the absorbance readings subtracted, as control for binding specificity. Figure 6 shows a significant percentage increase of anti-Aβ antibody absorbance value over non-immune control IgG in fAD conditioned medium, with respect to healthy controls.

Next, we analyzed the effects of NSC47924 inhibitor on Aβ levels in conditioned medium from healthy and fAD fibroblasts. The treatment with NSC47924 led to a reduction of the expression levels of Aβ in both healthy control and fAD cells (* $p < 0.05$).

Furthermore, besides the relocation of APP in the Golgi apparatus, we found that inhibitor treatment did not induce any accumulation of amyloid peptide inside fAD cells (Figure S1, bottom right panel, APP-6E10/Giantin).

3. Discussion

In this study, we investigated the effects of a specific inhibitor of 37/67kDa LR [33] on APP maturation and Aβ generation in fibroblasts from patients affected by familial Alzheimer's disease (carrying *PSEN2* M239V pathogenic mutation, fAD2, fAD3 or not fAD1), compared with healthy unaffected controls.

Fibroblasts have been employed as an in vitro model for neurological diseases [34], and particularly for AD [35–37].

Since fibroblasts are the most commonly used primary somatic cell type for the generation of induced pluripotent stem cells, we hope to obtain a better characterization of biological processes related to NSC47924 action on fAD patient cell lines, to plan subsequently, reprogram and differentiate patient fibroblasts. Comparison of the effects of different LR inhibitor molecules on different cell types that may be considered to be non-relevant for the disease, such as fibroblasts, or more relevant to the

disease, such as neurons differentiated from iPSCs, will allow us to develop more predictive in vitro systems for drug discovery. Our results obtained in fibroblasts represent the first step to reinforce the value of utilizing human iPSCs in drug discovery to improve translational predictability.

Previous studies have already reported a critical role for 37/67kDa LR in APP processing through direct interaction with the γ-secretases and indirect interaction with the β-secretase [38]. The role of 37/67kDa LR highlights the importance of identifying therapeutics that target the receptor [39], which has also been previously shown by us to be an interactor and regulator of prion protein trafficking [22,40,41]. In addition, our previous data showing the interaction between 37/67kDa LR and APP in mouse neuronal cells [10], together with the finding of regulation of APP maturation through receptor inhibition, prompted us to analyze the role of 37/67kDa LR in AD by challenging the specific receptor inhibitor NSC47924 (previously found active on prion protein trafficking) [22], with cells derived from fAD patients.

Protein maturation through the secretory pathway is strictly related to its intracellular trafficking. Since APP maturation is crucial for correct protein processing and coordination between the non-amyloidogenic and amyloidogenic pathway, we decided to test the effects of two LR inhibitors in pathological conditions, human cells derived from AD affected individuals.

After pilot experiments on APP using two different and previously selected analogs of LR inhibitors in mouse neuronal cells (NSC48478 and NSC47924) [10,22,33], only NSC47924 has been found to exert effects on trafficking and maturation of APP in human cells, restoring the "correct" ones that were lost in affected cells. Therefore, in the present study we decided to report only the active molecule NSC47924.

According to previous findings reporting the expression of APP as two major isoforms, corresponding to immature unglycosylated and mature modified isoform [10,42], we found APP migrating as two bands on SDS-PAGE. Differently from this observation, APP was expressed prevalently as an immature isoform in AD affected fibroblasts, suggesting an alternative trafficking pathway for APP in fAD cells with respect to unaffected cells.

Moreover, in line with other reports, where in physiological conditions, APP was localized in the Golgi apparatus [10,20,21,43], we found a prevalent distribution of APP in the Golgi of unAD cells. On the contrary, the APP is mainly colocalized with Tfr-positive recycling endosomes in the fAD fibroblast cell lines analyzed, suggesting a different trafficking pathway in disease conditions. This finding is extremely important if we consider previously reported data from Das et al., describing the convergence between the APP and the β-secretase BACE1 in recycling endosomes of neurons from brains with AD [44].

Interestingly, inhibition of 37/67kDa LR by NSC47924 was able to reverse the APP isoform ratio, restoring the levels almost to that of unAD cells.

APP modifications and trafficking are mutually regulated, contributing in turn to the modulation of Aβ generation [45]. The acquisition of APP post-translational modifications occurs mainly during the passage through the secretory pathway in neurons [42,46], where the protein can undergo glycosylation which starts in the ER to proceed through the Golgi, where sulfation and phosphorylation occur. Since we found that a reduced level of mature APP in AD-affected cells was accompanied by a mislocalization of the APP from the Golgi and consequent accumulation into recycling endosomes (Figure 3, Figures S1 and S2), we speculated that the APP was not able to be correctly modified for maturation probably because of its inability to transit through the secretory pathway and to reach the Golgi apparatus, where the majority of the APP modifications occurs.

Therefore, the possibility to control APP trafficking (by inhibiting the receptor LR, as well as we have previously done in neuronal cells) [10], would be reflected in APP maturation changing. Our hypothesis has been confirmed by showing that after inhibitor treatment, the APP recovered its Golgi localization and its molecular weight at the same level of unaffected cells (Figures 2 and 3).

Processing of the APP by α-, β- and γ-secretases generating APP-CTFs (C-terminal fragments) and Aβ, is strictly related to the subcellular localization and trafficking of APP. Because the secretases have

different distribution within the cells, the itinerary followed by the APP is crucial for determining the amount of APP fragments. Furthermore, CTFs have been found localized to subcellular microdomains between the ER and mitochondria [47], and they can lead, as well as Aβ, to mitochondrial dysfunction and morphology alteration in in vivo and in vitro AD study models [48–50]. According to findings in the literature, we observed an altered mitochondrial network in fAD cells. Therefore, we speculated that if in AD-affected cells we would be able (by using LR inhibitor) to reverse the subcellular localization of the APP and, consequently, its trafficking to that of healthy cells, we should have observed a restoring of cellular phenotype resembling one of healthy conditions, including mitochondrial network phenotype.

Given the key role of mitochondria in protein misfolding diseases [51,52], by means of immunofluorescence analysis on imaged fibroblasts, we have evaluated the mitochondrial network in terms of number and volume of mitochondria. In fAD cells, we observed a significant decrease of 3D objects volume and number, indicating mitochondrial dysfunction in disease conditions. Again, 37/67kDa LR inhibition almost completely rescued mitochondrial values to that of control fibroblasts by increasing both mitochondrial volume and number. This feature was accompanied by the finding of Akt inactivation and consequent pGSK3β decrease in fAD cells. Although several lines of evidence report increased activity of this enzyme in AD [32,53–55], we should acknowledge that direct evidence for this is still limited, since some studies find no change in GSK3 activity [56] or reduced GSK3 activity in AD [57].

Moreover, the ability of NSC47924 to "correct" the localization and maturation of APP and the consequent inactivation of the Akt pathway and regulation of GSK3β, can be critical for APP processing and reveal NSC47924 as a useful compound to be tested for Aβ production. Indeed, we challenged the inhibitor with fAD cells to test Aβ levels in cell culture media in comparison with unAD. Besides the fact that, as expected and previously found [58,59], the Aβ levels were higher in AD with respect to healthy conditions, the use of NSC47924 induced a significant decrease of Aβ levels in fAD. Furthermore, our finding that 37/67kDa LR inhibition did not induce any accumulation of amyloid peptide inside fAD cells, suggests that the reduction of Aβ in the cell culture media was likely due to impairment of Aβ production rather than to a lack of its secretion.

However, although further studies will be needed to validate 37/67kDa LR as a potential target for Alzheimer's disease, since NSC47924 is essentially intended to act on CNS, it will be interesting to challenge the inhibitor with in vivo conditions, where the cellular environment governs the pathophysiology of the disease.

4. Materials and Methods

4.1. Sanger Sequencing

The coding regions and the boundary intronic regions of *APP*, *PSEN1* and *PSEN2* genes we sequenced by direct Sanger sequencing, and 17, 11, and 10 primer pairs were designed to amplify the above-mentioned regions of *APP*, *PSEN1*, and *PSEN2*, respectively (Table S1). Genomic DNA was obtained by a pellet of at least 5×10^5 cells using the MasterPure Complete DNA purification kit (Epicentre Biotechnologies, Madison, WI, USA) following the manufacturer's instructions.

Each amplicon was individually amplified, assessed for quality on 2% agarose gel, and purified before sequencing reactions. Direct sequencing was performed with the ABI 3100 capillary sequencer (Applied Biosystems Inc., Foster City, CA, USA), and sequence data analysis was carried out using the SeqMan software (DNASTAR, Inc., Madison, WI, USA). Next, DNA variants were categorized accordingly to Ensembl (https://www.ensembl.org/index.html), ClinVar (https://www.ncbi.nlm.nih.gov/clinvar/) and dbSNP (https://www.ncbi.nlm.nih.gov/SNP/) databases and the possible impact of specific variations at the protein level was predicted using VarSome (https://varsome.com) and or Human Splicing Finder (http://www.umd.be/HSF/HSF.shtml) tools.

A full list of the primer pairs used to amplify *APP*, *PSEN1* and *PSEN2* genes are illustrated in Table S1.

4.2. Reagents and Antibodies

Cell culture reagents were purchased from Gibco Laboratories (Grand Island, NY, USA). Transferrin Alexa-594- conjugated (Tfr), cy2-, cy5-conjugated secondary Abs and Mitotracker Red CMXRos were from Invitrogen (Molecular Probes, Eugene, OR, USA). The anti-Giantin antibody was from StressGen Biotechnologies Corp (Victoria, BC, Canada). Anti-β-tubulin antibody was from Abcam. Anti-GSK, anti-pGSK3β Ser9 and DAPI were from Cell Signalling Technology. Anti-APP rabbit polyclonal antibody A8717 was from Sigma-Aldrich (St. Louis, MO, USA). Anti-Aβ antibody 6E10 (previously Covance, SIG-39320) and 4G8 were from Biolegend. All other reagents were from Sigma Chemical Co. (St. Louis, MO, USA). NSC47924 [1-((4-methoxyanilino)methyl)-2-naphtol] was obtained from the NCI/DTP Open Chemical repository (http://dtp.cancer.gov), dissolved in DMSO and stored at −20 °C.

4.3. Cell Culture and Drug Treatment

Fibroblasts were derived directly from the skin punch biopsy of the Italian patients carrying (fAD2: male with onset AD 48 years, and fAD3: female with onset AD 45 years) or not (fAD1, female, with unknown onset AD) the *PSEN2* M239V mutation. Written informed consent was obtained from each patient. All fibroblasts were derived from patients with a clinical diagnosis of probable early-onset fAD according to the criteria established by the Diagnostic and Statistical Manual of Mental Disorders (4th edition, DSM IV) [American Psychiatric Association, *Diagnostic and Statistical Manual of Mental Disorders*, American Psychiatric Association, Washington, DC, USA, 4th edition, 1994], the National Institute of Neurological and Communicative Disorders and Stroke, and reevaluated according to the NIA-Alzheimer's Association workgroups on diagnostic guidelines for AD [1]. The cells were grown in Dulbecco's modified Eagle's medium (DMEM), with 4500 mg/glucose/L, 110 mg sodium pyruvate and L-glutamine (SIGMA D6429), supplemented with 10% fetal bovine serum. For inhibitor NSC47924 treatment, the cells were washed in serum free medium, incubated for 30 min at room temperature in Areal medium (13.5 g/L of Dulbecco's modified eagle's medium with glutamine SIGMA-D-7777 without NaHCO$_3$, 0.2% BSA and 20 mM HEPES, final pH 7.5) and for further 24 h at 37 °C under 5% CO$_2$ in the presence of 20 μM inhibitor in DMEM supplemented with 1% serum. As control cells, fibroblasts from 2 unaffected individuals (unAD) were derived and grown in the same conditions. All the experiments were performed in 3 lines of fAD and 2 of unAD.

4.4. Indirect Immunofluorescence and Confocal Microscopy

Fibroblasts were cultured to 50% confluence in a growth medium, washed in PBS, fixed in 4% paraformaldehyde (PFA), permeabilized or not with 0.1% TX-100 for 30 min (where indicated) and processed for indirect immunofluorescence using specific antibodies 30 min in PBS/BSA 0.1%. The cells were incubated with rabbit anti-APP (A8718) antibody and markers of intracellular organelles, followed by incubation with fluorophore-conjugated secondary antibodies. When Tfr-Alexa594 was incubated in cell culture media, APP (labeled with cy2, visualized in green), and Giantin (labeled with cy5, blue channel but shown in red) were labelled with primary antibodies followed by cy2- and cy5-conjugated secondary antibodies, respectively. For easier visualization of the overlay channel, the pictures were elaborated after confocal microscopy acquisition, to split channels by rendering red the cy5 (blue) channel.

For mitochondrial staining, cells were incubated with Mitotracker Red CMXRos (500 nM) 20 min at 37 °C, before fixing with PFA and cold methanol 5 min on ice. Quantitative analysis was performed on a minimum of 30 cells by setting the same threshold of fluorescence intensity in all the samples analyzed. The mitochondrial network was then described in numbers of objects (ImageJ software) and object volume using the 3D object counter available in the software Fiji (http://www.fiji.sc).

For Tfr-Alexa 594 staining, the cells were incubated 30 min at 37 °C in complete medium before proceeding with immunofluorescence. Nuclei were stained by using DAPI (1:1000) in PBS.

Pearson's Correlation Coefficient (PCC) was employed to quantify colocalization [60] between APP and Giantin (as well as Tfr), and was determined in at least 25 cells from three different experiments. PCC was calculated in regions of APP and reference protein co-presence as previously described [10].

The PCC was then calculated in the defined regions for the images of interest. Immunofluorescences were analyzed by the confocal microscope LSM 700 Zeiss equipped with an oil immersion 63 × 1.4 NA Plan Apochromat objective (or 40×), and a pinhole size of one airy unit.

4.5. Direct ELISA for Detection of Aβ in Conditioned Medium from Human Skin Fibroblasts

High binding plates with 96 flat-bottomed wells (Corning, Amsterdam, The Netherlands) were coated with conditioned medium from healthy and AD human skin fibroblasts, or BSA as a negative control, and incubated at 4 °C overnight. After washing in PBS, residual binding sites were blocked for 1 h at 37 °C with 200 μL of blocking buffer (2% FCS, 1 mg/mL BSA, in PBS). Wells were incubated with 0.002 μg/mL of anti-β-Amyloid monoclonal antibodies (6E10 or 4G8) or non-immune control immunoglobulins for 1 h at room temperature. Each well was washed three times with wash buffer (0.5% Tween in PBS). HRP-conjugated goat anti-mouse secondary antibody (1:5000) was added for 1 h at room temperature. After washing in PBS, OPD (o-phenylenediamine dihydrochloride) substrate solution was added and absorbance was detected at 490 nm on an ELISA plate reader (Bio-Rad). Binding affinity was determined by subtracting background absorbance (BSA wells).

For experiments with NSC47924, healthy and fAD fibroblasts were incubated for 24 h at 37 °C. After treatment the conditioned media were collected and stored at −20 °C.

4.6. Statistical Analysis

Data are expressed as mean ± SD. All statistical analyses using two-way ANOVA and histograms were completed with excel software. Differences were considered statistically significant when $p < 0.05$.

Abbreviations

AD	Alzheimer's Disease
APP	amyloid precursor protein
Aβ	amyloid beta peptide
CTFs	C-terminal fragments
fAD	familial Alzheimer's disease
GSK3	Glycogen-synthase kinase 3
LR	laminin receptor

PCC   Pearson's Correlation Coefficient
PFA   Paraformaldehyde
PSEN1   Presenilin-1
PSEN2   Presenilin-2
Tfr   Transferrin
unAD   unaffected

References

1. McKhann, G.M.; Knopman, D.S.; Chertkow, H.; Hyman, B.T.; Jack, C.R., Jr.; Kawas, C.H.; Klunk, W.E.; Koroshetz, W.J.; Manly, J.J.; Mayeux, R.; et al. The diagnosis of dementia due to Alzheimer's disease: Recommendations from the National Institute on Aging-Alzheimer's Association workgroups on diagnostic guidelines for Alzheimer's disease. *Alzheimers Dement.* **2011**, *7*, 263–269. [CrossRef] [PubMed]

2. Benilova, I.; Karran, E.; De Strooper, B. The toxic Abeta oligomer and Alzheimer's disease: An emperor in need of clothes. *Nat. Neurosci.* **2012**, *15*, 349–357. [CrossRef] [PubMed]

3. D'Argenio, V.; Sarnataro, D. New Insights into the Molecular Bases of Familial Alzheimer's Disease. *J. Pers. Med.* **2020**, *10*, 26. [CrossRef] [PubMed]

4. Sherrington, R.; Rogaev, E.I.; Liang, Y.; Rogaeva, E.A.; Levesque, G.; Ikeda, M.; Chi, H.; Lin, C.; Li, G.; Holman, K.; et al. Cloning of a gene bearing missense mutations in early-onset familial Alzheimer's disease. *Nature* **1995**, *375*, 754–760. [CrossRef] [PubMed]

5. Levy-Lahad, E.; Wasco, W.; Poorkaj, P.; Romano, D.M.; Oshima, J.; Pettingell, W.H.; Yu, C.E.; Jondro, P.D.; Schmidt, S.D.; Wang, K.; et al. Candidate gene for the chromosome 1 familial Alzheimer's disease locus. *Science* **1995**, *269*, 973–977. [CrossRef]

6. Scheuner, D.; Eckman, C.; Jensen, M.; Song, X.; Citron, M.; Suzuki, N.; Bird, T.D.; Hardy, J.; Hutton, M.; Kukull, W.; et al. Secreted amyloid beta-protein similar to that in the senile plaques of Alzheimer's disease is increased in vivo by the presenilin 1 and 2 and APP mutations linked to familial Alzheimer's disease. *Nat. Med.* **1996**, *2*, 864–870. [CrossRef]

7. Hardy, J.; Selkoe, D.J. The amyloid hypothesis of Alzheimer's disease: Progress and problems on the road to therapeutics. *Science* **2002**, *297*, 353–356. [CrossRef]

8. Sarnataro, D. Attempt to Untangle the Prion-Like Misfolding Mechanism for Neurodegenerative Diseases. *Int. J. Mol. Sci.* **2018**, *19*, 3081. [CrossRef]

9. D'Argenio, V.; Sarnataro, D. Microbiome Influence in the Pathogenesis of Prion and Alzheimer's Diseases. *Int. J. Mol. Sci.* **2019**, *20*, 4704. [CrossRef]

10. Bhattacharya, A.; Limone, A.; Napolitano, F.; Cerchia, C.; Parisi, S.; Minopoli, G.; Montuori, N.; Lavecchia, A.; Sarnataro, D. APP Maturation and Intracellular Localization Are Controlled by a Specific Inhibitor of 37/67 kDa Laminin-1 Receptor in Neuronal Cells. *Int. J. Mol. Sci.* **2020**, *21*, 1738. [CrossRef]

11. Capell, A.; Meyn, L.; Fluhrer, R.; Teplow, D.B.; Walter, J.; Haass, C. Apical sorting of beta-secretase limits amyloid beta-peptide production. *J. Biol. Chem.* **2002**, *277*, 5637–5643. [CrossRef] [PubMed]

12. Andersen, O.M.; Reiche, J.; Schmidt, V.; Gotthardt, M.; Spoelgen, R.; Behlke, J.; von Arnim, C.A.; Breiderhoff, T.; Jansen, P.; Wu, X.; et al. Neuronal sorting protein-related receptor sorLA/LR11 regulates processing of the amyloid precursor protein. *Proc. Natl. Acad. Sci. USA* **2005**, *102*, 13461–13466. [CrossRef] [PubMed]

13. Schmidt, V.; Sporbert, A.; Rohe, M.; Reimer, T.; Rehm, A.; Andersen, O.M.; Willnow, T.E. SorLA/LR11 regulates processing of amyloid precursor protein via interaction with adaptors GGA and PACS-1. *J. Biol. Chem.* **2007**, *282*, 32956–32964. [CrossRef] [PubMed]

14. Toh, W.H.; Gleeson, P.A. Dysregulation of intracellular trafficking and endosomal sorting in Alzheimer's disease: Controversies and unanswered questions. *Biochem. J.* **2016**, *473*, 1977–1993. [CrossRef] [PubMed]

15. Tan, J.Z.A.; Gleeson, P.A. The role of membrane trafficking in the processing of amyloid precursor protein and production of amyloid peptides in Alzheimer's disease. *Biochim. Biophys. Acta Biomembr.* **2019**, *1861*, 697–712. [CrossRef]

16. Da Costa Dias, B.; Jovanovic, K.; Gonsalves, D.; Moodley, K.; Reusch, U.; Knackmuss, S.; Weinberg, M.S.; Little, M.; Weiss, S.F. The 37kDa/67kDa laminin receptor acts as a receptor for Abeta42 internalization. *Sci. Rep.* **2014**, *4*, 5556. [CrossRef]

17. Pinnock, E.C.; Jovanovic, K.; Pinto, M.G.; Ferreira, E.; Dias Bda, C.; Penny, C.; Knackmuss, S.; Reusch, U.; Little, M.; Schatzl, H.M.; et al. LRP/LR Antibody Mediated Rescuing of Amyloid-beta-Induced Cytotoxicity is Dependent on PrPc in Alzheimer's Disease. *J. Alzheimers Dis.* **2016**, *49*, 645–657. [CrossRef]

18. Cacace, R.; Sleegers, K.; Van Broeckhoven, C. Molecular genetics of early-onset Alzheimer's disease revisited. *Alzheimers Dement.* **2016**, *12*, 733–748. [CrossRef]

19. Haass, C.; Kaether, C.; Thinakaran, G.; Sisodia, S. Trafficking and proteolytic processing of APP. *Cold Spring Harb. Perspect. Med.* **2012**, *2*, a006270. [CrossRef]

20. Tam, J.H.; Seah, C.; Pasternak, S.H. The Amyloid Precursor Protein is rapidly transported from the Golgi apparatus to the lysosome and where it is processed into beta-amyloid. *Mol. Brain* **2014**, *7*, 54. [CrossRef]

21. Tan, J.Z.A.; Gleeson, P.A. The trans-Golgi network is a major site for alpha-secretase processing of amyloid precursor protein in primary neurons. *J. Biol. Chem.* **2019**, *294*, 1618–1631. [CrossRef] [PubMed]

22. Sarnataro, D.; Pepe, A.; Altamura, G.; De Simone, I.; Pesapane, A.; Nitsch, L.; Montuori, N.; Lavecchia, A.; Zurzolo, C. The 37/67 kDa laminin receptor (LR) inhibitor, NSC47924, affects 37/67 kDa LR cell surface localization and interaction with the cellular prion protein. *Sci. Rep.* **2016**, *6*, 24457. [CrossRef] [PubMed]

23. Colavita, I.; Nigro, E.; Sarnataro, D.; Scudiero, O.; Granata, V.; Daniele, A.; Zagari, A.; Pessi, A.; Salvatore, F. Membrane protein 4F2/CD98 is a cell surface receptor involved in the internalization and trafficking of human beta-Defensin 3 in epithelial cells. *Chem. Biol.* **2015**, *22*, 217–228. [CrossRef] [PubMed]

24. Hirai, K.; Aliev, G.; Nunomura, A.; Fujioka, H.; Russell, R.L.; Atwood, C.S.; Johnson, A.B.; Kress, Y.; Vinters, H.V.; Tabaton, M.; et al. Mitochondrial abnormalities in Alzheimer's disease. *J. Neurosci.* **2001**, *21*, 3017–3023. [CrossRef] [PubMed]

25. Calkins, M.J.; Manczak, M.; Mao, P.; Shirendeb, U.; Reddy, P.H. Impaired mitochondrial biogenesis, defective axonal transport of mitochondria, abnormal mitochondrial dynamics and synaptic degeneration in a mouse model of Alzheimer's disease. *Hum. Mol. Genet.* **2011**, *20*, 4515–4529. [CrossRef]

26. Cenini, G.; Voos, W. Mitochondria as Potential Targets in Alzheimer Disease Therapy: An Update. *Front. Pharmacol.* **2019**, *10*, 902. [CrossRef]

27. Mollo, N.; Cicatiello, R.; Aurilia, M.; Scognamiglio, R.; Genesio, R.; Charalambous, M.; Paladino, S.; Conti, A.; Nitsch, L.; Izzo, A. Targeting Mitochondrial Network Architecture in Down Syndrome and Aging. *Int. J. Mol. Sci.* **2020**, *21*, 3134. [CrossRef]

28. Izzo, A.; Nitti, M.; Mollo, N.; Paladino, S.; Procaccini, C.; Faicchia, D.; Cali, G.; Genesio, R.; Bonfiglio, F.; Cicatiello, R.; et al. Metformin restores the mitochondrial network and reverses mitochondrial dysfunction in Down syndrome cells. *Hum. Mol. Genet.* **2017**, *26*, 1056–1069. [CrossRef]

29. Chan, D.C. Fusion and fission: Interlinked processes critical for mitochondrial health. *Annu. Rev. Genet.* **2012**, *46*, 265–287. [CrossRef]

30. Yang, K.; Chen, Z.; Gao, J.; Shi, W.; Li, L.; Jiang, S.; Hu, H.; Liu, Z.; Xu, D.; Wu, L. The Key Roles of GSK-3beta in Regulating Mitochondrial Activity. *Cell. Physiol. Biochem.* **2017**, *44*, 1445–1459. [CrossRef]

31. Gleyzer, N.; Scarpulla, R.C. Concerted Action of PGC-1-related Coactivator (PRC) and c-MYC in the Stress Response to Mitochondrial Dysfunction. *J. Biol. Chem.* **2016**, *291*, 25529–25541. [CrossRef] [PubMed]

32. Leroy, K.; Yilmaz, Z.; Brion, J.P. Increased level of active GSK-3beta in Alzheimer's disease and accumulation in argyrophilic grains and in neurones at different stages of neurofibrillary degeneration. *Neuropathol. Appl. Neurobiol.* **2007**, *33*, 43–55. [CrossRef] [PubMed]

33. Pesapane, A.; Di Giovanni, C.; Rossi, F.W.; Alfano, D.; Formisano, L.; Ragno, P.; Selleri, C.; Montuori, N.; Lavecchia, A. Discovery of new small molecules inhibiting 67 kDa laminin receptor interaction with laminin and cancer cell invasion. *Oncotarget* **2015**, *6*, 18116–18133. [CrossRef] [PubMed]

34. Connolly, G.P. Fibroblast models of neurological disorders: Fluorescence measurement studies. *Trends Pharmacol. Sci.* **1998**, *19*, 171–177. [CrossRef]

35. Gasparini, L.; Racchi, M.; Binetti, G.; Trabucchi, M.; Solerte, S.B.; Alkon, D.; Etcheberrigaray, R.; Gibson, G.; Blass, J.; Paoletti, R.; et al. Peripheral markers in testing pathophysiological hypotheses and diagnosing Alzheimer's disease. *FASEB J.* **1998**, *12*, 17–34. [CrossRef]

36. Govoni, S.; Gasparini, L.; Racchi, M.; Trabucchi, M. Peripheral cells as an investigational tool for Alzheimer's disease. *Life Sci.* **1996**, *59*, 461–468. [CrossRef]

37. Mocali, A.; Della Malva, N.; Abete, C.; Mitidieri Costanza, V.A.; Bavazzano, A.; Boddi, V.; Sanchez, L.; Dessi, S.; Pani, A.; Paoletti, F. Altered proteolysis in fibroblasts of Alzheimer patients with predictive implications for subjects at risk of disease. *Int. J. Alzheimers Dis.* **2014**, *2014*, 520152. [CrossRef]

38. Jovanovic, K.; Loos, B.; Da Costa Dias, B.; Penny, C.; Weiss, S.F. High resolution imaging study of interactions between the 37 kDa/67 kDa laminin receptor and APP, beta-secretase and gamma-secretase in Alzheimer's disease. *PLoS ONE* **2014**, *9*, e100373. [CrossRef]

39. Jovanovic, K.; Chetty, C.J.; Khumalo, T.; Da Costa Dias, B.; Ferreira, E.; Malindisa, S.T.; Caveney, R.; Letsolo, B.T.; Weiss, S.F. Novel patented therapeutic approaches targeting the 37/67 kDa laminin receptor for treatment of cancer and Alzheimer's disease. *Expert Opin. Ther. Pat.* **2015**, *25*, 567–582. [CrossRef]

40. Sarnataro, D.; Pepe, A.; Zurzolo, C. Cell Biology of Prion Protein. *Prog. Mol. Biol. Transl. Sci.* **2017**, *150*, 57–82. [CrossRef]

41. Pepe, A.; Avolio, R.; Matassa, D.S.; Esposito, F.; Nitsch, L.; Zurzolo, C.; Paladino, S.; Sarnataro, D. Regulation of sub-compartmental targeting and folding properties of the Prion-like protein Shadoo. *Sci. Rep.* **2017**, *7*, 3731. [CrossRef] [PubMed]

42. Walter, J.; Haass, C. Posttranslational modifications of amyloid precursor protein: Ectodomain phosphorylation and sulfation. *Methods Mol. Med.* **2000**, *32*, 149–168. [CrossRef] [PubMed]

43. Tan, J.Z.A.; Fourriere, L.; Wang, J.; Perez, F.; Boncompain, G.; Gleeson, P.A. Distinct anterograde trafficking pathways of BACE1 and amyloid precursor protein from the TGN and the regulation of amyloid-beta production. *Mol. Biol. Cell* **2020**, *31*, 27–44. [CrossRef] [PubMed]

44. Das, U.; Scott, D.A.; Ganguly, A.; Koo, E.H.; Tang, Y.; Roy, S. Activity-induced convergence of APP and BACE-1 in acidic microdomains via an endocytosis-dependent pathway. *Neuron* **2013**, *79*, 447–460. [CrossRef] [PubMed]

45. Wang, X.; Zhou, X.; Li, G.; Zhang, Y.; Wu, Y.; Song, W. Modifications and Trafficking of APP in the Pathogenesis of Alzheimer's Disease. *Front. Mol. Neurosci.* **2017**, *10*, 294. [CrossRef] [PubMed]

46. DelBove, C.E.; Deng, X.Z.; Zhang, Q. The Fate of Nascent APP in Hippocampal Neurons: A Live Cell Imaging Study. *ACS Chem. Neurosci.* **2018**, *9*, 2225–2232. [CrossRef]

47. Del Prete, D.; Suski, J.M.; Oules, B.; Debayle, D.; Gay, A.S.; Lacas-Gervais, S.; Bussiere, R.; Bauer, C.; Pinton, P.; Paterlini-Brechot, P.; et al. Localization and Processing of the Amyloid-beta Protein Precursor in Mitochondria-Associated Membranes. *J. Alzheimers Dis.* **2017**, *55*, 1549–1570. [CrossRef]

48. Anandatheerthavarada, H.K.; Devi, L. Amyloid precursor protein and mitochondrial dysfunction in Alzheimer's disease. *Neuroscientist* **2007**, *13*, 626–638. [CrossRef]

49. Reddy, P.H.; Beal, M.F. Amyloid beta, mitochondrial dysfunction and synaptic damage: Implications for cognitive decline in aging and Alzheimer's disease. *Trends Mol. Med.* **2008**, *14*, 45–53. [CrossRef]

50. Vaillant-Beuchot, L.; Mary, A.; Pardossi-Piquard, R.; Bourgeois, A.; Lauritzen, I.; Eysert, F.; Kinoshita, P.F.; Cazareth, J.; Badot, C.; Fragaki, K.; et al. Accumulation of amyloid precursor protein C-terminal fragments triggers mitochondrial structure, function, and mitophagy defects in Alzheimer's disease models and human brains. *Acta Neuropathol.* **2020**, 1–27. [CrossRef]

51. Balaban, R.S.; Nemoto, S.; Finkel, T. Mitochondria, oxidants, and aging. *Cell* **2005**, *120*, 483–495. [CrossRef] [PubMed]

52. Jeong, S. Molecular and Cellular Basis of Neurodegeneration in Alzheimer's Disease. *Mol. Cells* **2017**, *40*, 613–620. [CrossRef] [PubMed]

53. Hooper, C.; Killick, R.; Lovestone, S. The GSK3 hypothesis of Alzheimer's disease. *J. Neurochem.* **2008**, *104*, 1433–1439. [CrossRef]

54. Pei, J.J.; Braak, E.; Braak, H.; Grundke-Iqbal, I.; Iqbal, K.; Winblad, B.; Cowburn, R.F. Distribution of active glycogen synthase kinase 3beta (GSK-3beta) in brains staged for Alzheimer disease neurofibrillary changes. *J. Neuropathol. Exp. Neurol.* **1999**, *58*, 1010–1019. [CrossRef] [PubMed]

55. Ochalek, A.; Mihalik, B.; Avci, H.X.; Chandrasekaran, A.; Teglasi, A.; Bock, I.; Giudice, M.L.; Tancos, Z.; Molnar, K.; Laszlo, L.; et al. Neurons derived from sporadic Alzheimer's disease iPSCs reveal elevated TAU hyperphosphorylation, increased amyloid levels, and GSK3B activation. *Alzheimers Res. Ther.* **2017**, *9*, 90. [CrossRef] [PubMed]

56. Pei, J.J.; Tanaka, T.; Tung, Y.C.; Braak, E.; Iqbal, K.; Grundke-Iqbal, I. Distribution, levels, and activity of glycogen synthase kinase-3 in the Alzheimer disease brain. *J. Neuropathol. Exp. Neurol.* **1997**, *56*, 70–78. [CrossRef] [PubMed]

57. Swatton, J.E.; Sellers, L.A.; Faull, R.L.; Holland, A.; Iritani, S.; Bahn, S. Increased MAP kinase activity in Alzheimer's and Down syndrome but not in schizophrenia human brain. *Eur. J. Neurosci.* **2004**, *19*, 2711–2719. [CrossRef] [PubMed]

58. Martins, R.N.; Turner, B.A.; Carroll, R.T.; Sweeney, D.; Kim, K.S.; Wisniewski, H.M.; Blass, J.P.; Gibson, G.E.; Gandy, S. High levels of amyloid-beta protein from S182 (Glu246) familial Alzheimer's cells. *Neuroreport* **1995**, *7*, 217–220. [CrossRef]

59. Citron, M.; Vigo-Pelfrey, C.; Teplow, D.B.; Miller, C.; Schenk, D.; Johnston, J.; Winblad, B.; Venizelos, N.; Lannfelt, L.; Selkoe, D.J. Excessive production of amyloid beta-protein by peripheral cells of symptomatic and presymptomatic patients carrying the Swedish familial Alzheimer disease mutation. *Proc. Natl. Acad. Sci. USA* **1994**, *91*, 11993–11997. [CrossRef]

60. Bolte, S.; Cordelieres, F.P. A guided tour into subcellular colocalization analysis in light microscopy. *J. Microsc.* **2006**, *224*, 213–232. [CrossRef]